SEMARAK ILMU PUBLISHING

Journal of Advanced Research in Fluid Mechanics and Thermal Sciences

Journal homepage:
https://semarakilmu.com.my/journals/index.php/fluid_mechanics_thermal_sciences/index
ISSN: 2289-7879

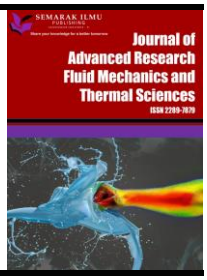

Unsteady Hiemenz Flow of Cu-SiO_2 Hybrid Nanofluid with Heat Generation/Absorption

Yap Bing Kho[1], Rahimah Jusoh[1,*], Mikhail Sheremet[2], Mohd Zuki Salleh[1], Zulkhibri Ismail[1], Nooraini Zainuddin[3]

[1] Centre for Mathematical Sciences, Universiti Malaysia Pahang Al-Sultan Abdullah, Lebuhraya Persiaran Tun Khalil Yaakob, 26300 Kuantan, Pahang, Malaysia
[2] Laboratory of Convective Heat and Mass Transfer, Tomsk State University, Tomsk, Russia
[3] Department of Fundamental & Applied Sciences, Universiti Teknologi PETRONAS, 32610 Bandar Seri Iskandar, Perak, Malaysia

ARTICLE INFO

Article history:
Received 10 July 2023
Received in revised form 28 September 2023
Accepted 10 October 2023
Available online 22 October 2023

Keywords:
Hybrid nanofluid; unsteady; Hiemenz flow; heat generation/absorption

ABSTRACT

The use of hybrid nanofluid as an alternate heat transfer fluid has shown great potential, and ongoing research to improve its thermal conductivity is important. This study focuses on the impact of heat generation/ absorption on the unsteady Hiemenz flow of aqueous hybrid nanofluid containing copper and silica nanoparticles. Mathematical equations for the hybrid nanofluid model are derived using suitable similarity transformations and solved numerically using bvp4c codes in Matlab software. The results indicate that increased heat generation/absorption leads to an increase in both momentum and thermal boundary layer thickness. The effects of suction and nanoparticle concentration are also analysed and presented graphically. Additionally, a stability analysis is also performed, which discloses that the first solution produced is stable, however, the second solution is not. The findings of this study provide valuable insights into the behaviour of hybrid nanofluid in unsteady flow and can aid in the development of more efficient heat transfer fluids for various engineering applications.

1. Introduction

In many practical engineering and natural phenomena, the flow is not always steady, but instead exhibits variations with respect to time. This unsteadiness can arise from various factors such as time-varying boundary conditions, fluctuating external forces, or inherent instabilities in the flow. Unsteady boundary layer flow research provides useful comprehensions into transitory behaviour, dynamic response, and time-dependent characteristics of the flow. For instance, the concept of unsteady flow can be seen in the dynamic pressure exchanger, aircraft wings, dynamic response of turbomachinery components, sediment transport in rivers and coastal areas, and particle dispersal by blast waves [1,2]. Bilal *et al.,* [3] investigated the radiation effect on the unsteady boundary layer flow and found that the increment of the unsteadiness parameter enhanced the fluid temperature.

* *Corresponding author.*
E-mail address: rahimahj@umpsa.edu.my

https://doi.org/10.37934/arfmts.110.2.95107

The Hiemenz flow, which involves fluid motion close to the stagnation area, was also extensively researched. Kandasamy *et al.,* [4] numerically studied the unsteady Hiemenz flow of nanofluid throughout a wedge by using the Lie group transformation. They found that the thermal boundary layer thickness thickened as the inclination angle increased. Mahmood *et al.,* [5] presented dual solutions for Hiemenz flow of micropolar fluid with magnetic effect. Dual solutions also had been revealed by Waini *et al.,* [6] for the Hiemenz flow of Al_2O_3-Cu hybrid nanofluid.

For centuries, researchers and engineers in the field of thermal engineering have dedicated significant efforts to enhance the properties of base fluids as effective heat transfer mediums. Traditional heat transfer fluids, such as water or oil, have limitations in terms of their thermal conductivity and heat transfer capabilities. These fluids may not be able to effectively dissipate heat from high-power systems or achieve efficient thermal management in various applications. To overcome these limitations, researchers have explored the concept of nanofluids, which are suspensions of nanoparticles in a base fluid. Nanoparticles, with their small size and high surface area-to-volume ratio, exhibit enhanced thermal properties that can lead to a substantial augmentation in the heat transfer efficiency of the base fluid. The scrutinization of nanofluid flow and heat transfer was conducted with consideration of various factors [7-9]. However, despite the advantages of nanofluids, there are challenges associated with their stability, particle aggregation, and cost-effectiveness. Researchers have been actively investigating ways to optimize the nanoparticle dispersion, mitigate particle agglomeration, and develop scalable synthesis methods to ensure the practical applicability of nanofluids. In recent years, the concept of hybrid nanofluids has emerged as an innovative approach to further enhance heat transfer performance. Hybrid nanofluids involve the combination of different types of nanoparticles or even other additives with the base fluid. Khan *et al.,* [10] explored the unsteady stagnation point flow of Ag-TiO_2 hybrid nanofluid and observed an increase in temperature based on their model. Conversely, Maiti *et al.,* [11] obtained contrasting results in their study of unsteady stagnation Al_2O_3-Cu hybrid nanofluid, where they found a decrease in temperature when incorporating the magnetic parameter. Lahari *et al.,* [12] researched the Cu-SiO_2 hybrid nanofluid with glycerine water as the base fluid and discovered that the dynamic viscosity rose as the volume concentration increased. This conclusion is consistent with the findings of Dezfulizadeh *et al.,* [13] who conducted experimental research on Cu-SiO2-MWCN hybrid nanofluid.

Moreover, researchers have also taken into account the influences of heat generation/absorption. This phenomenon pertains to the generation or absorption of heat within the boundary layer of a fluid flow. Heat generation occurs when there is a local source or release of heat energy within the boundary layer. This can be due to various factors such as chemical reactions, electrical dissipation, frictional heating, or external heat sources. On the other hand, heat absorption involves the removal or absorption of heat energy from the fluid within the boundary layer. This can occur through mechanisms such as evaporation, phase change, or heat removal to a cooler surface. Masood *et al.,* [14] included the impact of heat generation/absorption in the polystyrene-TiO_2 hybrid nanofluid model and discovered the enlargement of temperature profiles. The same result also had been presented by Yasir *et al.,* [15] for Zn−TiO_2 hybrid nanofluid model. In addition, Rashad *et al.,* [16] concluded that the process of heat transfer increased with the inclusion of heat generation/absorption in the Eyring–Powell hybrid nanofluid model. Iftikhar *et al.,* [17] explored SiO_2-Cu hybrid nanofluid and found that the temperature and velocity significantly rise due to an increase in heat absorption.

Building upon the aforementioned studies, the objective of this current investigation is to explore the effects of heat generation/absorption on the unsteady Hiemenz flow of a hybrid nanofluid. Specifically, the hybrid nanofluid considered in this study is composed of a combination of copper

(Cu) nanoparticles and silicon dioxide/silica (SiO_2) nanoparticles, with water acting as the base fluid. The key focus of this study is to examine the enhancement of heat transfer achieved by utilizing a hybrid nanofluid, and to investigate the influence of key factors such as the unsteadiness parameter, suction, and the presence of heat sink/source on the behavior of the hybrid nanofluid flow. The comprehensive examination of these factors and their interactions will contribute to the understanding of heat transfer mechanisms and aiding in the development of efficient thermal management systems.

2. Problem Formulations

The formulation of Cu-SiO_2 hybrid nanofluid is initiated with the configuration of the physical model. In this study, we investigate the characteristics of an unsteady Hiemenz flow and heat transfer phenomenon involving the hybrid nanofluid This occurs in the region where $y > 0$ and is initiated by a stretching/shrinking surface that is impulsively started. The configuration of this system is depicted in Figure 1, where the Cartesian coordinates *x* and *y* represent measurements along the surface and orthogonal to it, respectively.

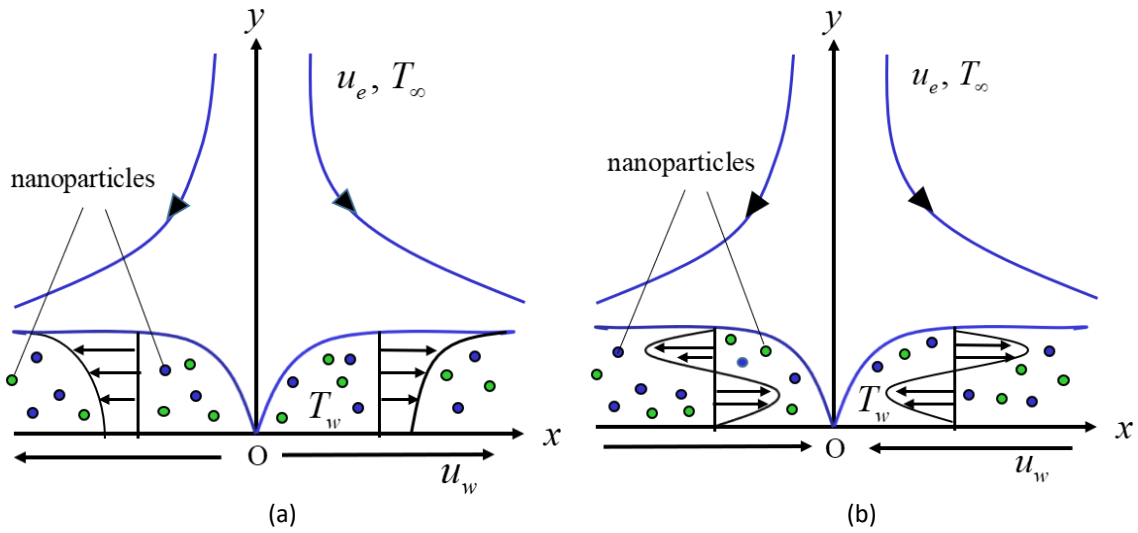

Fig. 1. Physical configuration of unsteady Hiemenz flow of hybrid nanofluid (a) Stretching sheet (b) Shrinking sheet

In this model, $u_e(x,t) = ax/1-ct$ denotes the velocity of the free stream, with $a > 0$ representing the intensity of the stagnation flow. The parameter *c* represents the degree of unsteadiness in the problem. On the other hand, the velocity associated with the stretching/shrinking motion is represented as $u_w(x,t) = bx/1-ct$, where *b* is a constant indicating stretching $(b > 0)$ or shrinking $(b < 0)$ occurrences.

Furthermore, we assume that the mass flux velocity is $v_w(x,t) = -\sqrt{av_f/1-ct}\, s$ where *s* denotes the constant mass flux velocity with $s > 0$ indicating suction and $s < 0$ indicating injection. The surface maintains a uniform temperature of T_w, while the surrounding fluid has a temperature of T_∞. It is important to note that in this scenario, we consider T_w to be greater than T_∞, indicating a heated surface. We also consider the heat generation/absorption effect with $Q_s = Q_0/1-ct$ where Q_0 represents the initial value of the heat generation/absorption. The governing equations for the

boundary layer flow of Cu-SiO_2 hybrid nanofluid, taking into account continuity, momentum, and energy, can be expressed as follows [16,18,19]:

$$\frac{\partial u}{\partial x}+\frac{\partial v}{\partial y}=0, \tag{1}$$

$$\frac{\partial u}{\partial t}+u\frac{\partial u}{\partial x}+v\frac{\partial u}{\partial y}=\frac{\partial u_e}{\partial t}+u_e\frac{\partial u_e}{\partial x}+\frac{\mu_{hnf}}{\rho_{hnf}}\frac{\partial^2 u}{\partial y^2}, \tag{2}$$

$$\frac{\partial T}{\partial t}+u\frac{\partial T}{\partial x}+v\frac{\partial T}{\partial y}=\alpha_{hnf}\frac{\partial^2 T}{\partial y^2}+\frac{Q_s\left(T-T_\infty\right)}{\left(\rho C_p\right)_{hnf}} \tag{3}$$

subject to the fulfillment of specific boundary conditions

$$\begin{aligned} &t<0: \quad u=v=0 \qquad \text{for any } x,y,\\ &t\geq 0: \quad u=u_w, \quad v=v_w \quad T=T_w \quad \text{at} \quad y=0,\\ &\qquad\quad u\to u_e, \qquad T\to T_\infty, \qquad\quad \text{as} \quad y\to\infty. \end{aligned} \tag{4}$$

The governing Eq. (1) to Eq. (3), which are associated with the boundary conditions (4), can be written in a simpler form by incorporating the following similarity transformations:

$$\eta=\sqrt{\frac{a}{\nu_f\left(1-ct\right)}}\,y, \quad u=\frac{ax}{1-ct}\,f'(\eta), \quad v=-\sqrt{\frac{a\nu_f}{1-ct}}\,f(\eta), \quad \theta(\eta)=\frac{T-T_\infty}{T_w-T_\infty}. \tag{5}$$

As a result, Eq. (1) is automatically satisfied, and Eq. (2) and Eq. (3) are then transformed into the following set of ordinary differential equations:

$$\frac{\mu_{hnf}/\mu_f}{\rho_{hnf}/\rho_f}f'''+ff''+\chi\left(1-f'-\frac{\eta}{2}f''\right)+1-f'^2=0, \tag{6}$$

$$\frac{k_{hnf}/k_f}{\Pr\left(\rho C_p\right)_{hnf}/\left(\rho C_p\right)_f}\theta''+f\theta'-\frac{1}{2}\chi\eta\theta'+\frac{Q\theta}{\left(\rho C_p\right)_{hnf}/\left(\rho C_p\right)_f}=0, \tag{7}$$

with the boundary conditions

$$\begin{aligned} &f(0)=s, \quad f'(0)=\lambda, \quad \theta(0)=1,\\ &f'(\eta)\to 1, \quad \theta(\eta)\to 0 \quad \text{as} \quad \eta\to\infty. \end{aligned} \tag{8}$$

In the aforementioned equations, Prandtl number Pr, unsteadiness parameter χ, stretching/shrinking parameter λ and heat source /sink *Q* are formulated as

$$\Pr = \frac{\nu_f}{\alpha_f}, \qquad \chi = \frac{c}{a}, \qquad \lambda = \frac{b}{a}, \qquad Q = \frac{Q_0}{a\left(\rho C_p\right)_f}, \tag{9}$$

where $Q > 0$ indicates the heat source while $Q < 0$ indicates heat sink.

The thermophysical properties of the hybrid nanofluid are described by additional parameters μ_{hnf}, α_{hnf}, ρ_{hnf}, $(\rho C_p)_{hnf}$, and k_{hnf}, characterizing dynamic viscosity, thermal diffusivity, density, heat capacity, and thermal conductivity, respectively. These properties are detailed in Table 1, which provides the formulas for the hybrid nanofluid characteristics. In the table, subscript *s*1 stands for copper nanoparticles, while subscript *s*2 stands for silicon dioxide or silica nanoparticles. The basic fluid, denoted by the subscript *f*, is water (H_2O), whereas the letters *nf* represents the nanofluid, and *hnf* signifies the hybrid nanofluid. The symbol of ϕ_{hnf} stands for the volume concentration of two types of disseminated nanoparticles in the hybrid nanofluid which can be defined as $\phi_{hnf} = \phi_1 + \phi_2$ [20]. For easy reference, Table 2 presents the thermophysical properties of water, as well as copper and silica nanoparticles.

Table 1
Formulations of hybrid nanofluid properties [20]

Properties	Nanofluid	Hybrid nanofluid
Density	$\rho_{nf} = (1-\phi_1)\rho_f + \phi_1\rho_s$	$\rho_{hnf} = \left(1-\phi_{hnf}\right)\rho_f + \phi_1\rho_{s1} + \phi_2\rho_{s2}$
Heat capacity	$\left(\rho C_p\right)_{nf} = (1-\phi_1)\left(\rho C_p\right)_f + \phi_1\left(\rho C_p\right)_s$	$\left(\rho C_p\right)_{hnf} = \left(1-\phi_{hnf}\right)\left(\rho C_p\right)_f + \phi_1\left(\rho C_p\right)_{s1} + \phi_2\left(\rho C_p\right)_{s2}$
Dynamic viscosity	$\mu_{nf} = \frac{\mu_f}{(1-\phi_1)^{2.5}}$	$\frac{\mu_{hnf}}{\mu_f} = \frac{1}{\left(1-\phi_{hnf}\right)^{2.5}}$
Thermal Conductivity	$k_{nf} = \frac{k_s + 2k_f - 2\phi_1\left(k_f - k_s\right)}{k_s + 2k_f + \phi_1\left(k_f - k_s\right)} \times k_f$	$\frac{k_{hnf}}{k_f} = \frac{\left(\frac{\phi_1 k_{s1} + \phi_2 k_{s2}}{\phi_{hnf}}\right) + 2k_f + 2\left(\phi_1 k_{s1} + \phi_2 k_{s2}\right) - 2\phi_{hnf} k_f}{\left(\frac{\phi_1 k_{s1} + \phi_2 k_{s2}}{\phi_{hnf}}\right) + 2k_f - \left(\phi_1 k_{s1} + \phi_2 k_{s2}\right) + \phi_{hnf} k_f}$

Table 2
Nanoparticles and base fluid thermophysical traits [21,22]

Properties	$\rho\left(kgm^{-3}\right)$	$C_p\left(Jkg^{-1}K^{-1}\right)$	$k\left(Wm^{-1}K^{-1}\right)$
Copper (Cu)	8933	385	401
Silicon Dioxide (SiO_2)	2650	730	1.5
H_2O	997.1	4179	0.613

The quantities of interest in this particular problem are the skin friction coefficient C_f and the Nusselt number Nu_x, both of which can be defined as follows:

$$C_f = \frac{\tau_w}{\rho_f u_e^2}, \qquad Nu_x = \frac{x\, q_w}{k_f\left(T_w - T_\infty\right)}, \tag{10}$$

where τ_w and q_w are the surface shear stress and the surface heat flux, respectively, which are defined as

$$\tau_{wx} = \mu_{hnf}\left(\frac{\partial u}{\partial y}\right)_{y=0}, \quad q_w = -k_{hnf}\left(\frac{\partial T}{\partial y}\right)_{y=0}. \tag{11}$$

Implementing Eq. (5), Eq. (10) and Eq. (11), we obtain

$$\sqrt{\mathrm{Re}_x}C_f = \frac{\mu_{hnf}}{\mu_f} f''(0), \qquad \sqrt{1/\mathrm{Re}_x}Nu_x = -\frac{k_{hnf}}{k_f}\theta'(0), \tag{12}$$

where $\mathrm{Re}_x = \frac{u_e x}{\nu_f}$ signifies the local Reynolds number.

3. Stability Analysis

Merkin [23] demonstrated the existence of dual solutions and emphasized the importance of stability analysis in determining the physically applicable solution, particularly for steady-state problems. Building on this idea, the concept of a dimensionless time variable, τ, which plays a crucial role in determining the physically meaningful solution is applied [24-26]. Therefore, to account for this dimensionless time variable, the variables (5) are altered, and new similarity variables are introduced, as follows:

$$\begin{aligned} &u = \frac{ax}{1-ct}\frac{\partial f}{\partial \eta}(\eta,\tau), \qquad v = -\sqrt{\frac{a\nu_f}{1-ct}}\,\big(f(\eta,\tau)\big), \\ &\theta(\eta,\tau) = \frac{T-T_\infty}{T_w-T_\infty}, \qquad \eta = \sqrt{\frac{a}{\nu_f(1-ct)}}\,y, \qquad \tau = \frac{at}{1-ct}. \end{aligned} \tag{13}$$

The following equations are produced by implementing similarity variables (13) to Eq. (2) and Eq. (3):

$$\frac{\mu_{hnf}/\mu_f}{\rho_{hnf}/\rho_f}\frac{\partial^3 f}{\partial \eta^3} + f\frac{\partial^2 f}{\partial \eta^2} + \chi\left(1-\frac{\partial f}{\partial \eta}-\frac{\eta}{2}\frac{\partial^2 f}{\partial \eta^2}\right)+1-\left(\frac{\partial f}{\partial \eta}\right)^2 - (1+\chi\tau)\frac{\partial^2 f}{\partial \eta \partial \tau} = 0, \tag{14}$$

$$\frac{k_{hnf}/k_f}{\mathrm{Pr}\left(\rho C_p\right)_{hnf}/\left(\rho C_p\right)_f}\frac{\partial^2 \theta}{\partial \eta^2} + \frac{Q\theta}{\left(\rho C_p\right)_{hnf}/\left(\rho C_p\right)_f} + f\frac{\partial \theta}{\partial \eta} - \frac{1}{2}\chi\eta\frac{\partial \theta}{\partial \eta} - (1+\chi\tau)\frac{\partial \theta}{\partial \tau} = 0, \tag{15}$$

pertaining to the boundary conditions

$$f(0,\tau) = s, \quad \frac{\partial f}{\partial \eta}(0,\tau) = \lambda \qquad \theta(0,\tau) = 1, \qquad \frac{\partial f}{\partial \eta}(\infty,\tau) \to 1, \qquad \theta(\infty,\tau) \to 0. \tag{16}$$

Next, following Weidman *et al.,* [26], we consider:

$$f(\eta,\tau)=f_0(\eta)+e^{-\gamma\tau}F(\eta),\qquad \theta(\eta,\tau)=\theta_0(\eta)+e^{-\gamma\tau}G(\eta). \tag{17}$$

The following equations are produced by replacing Eq. (17) into Eq. (14) and Eq. (15):

$$\frac{\mu_{hnf}/\mu_f}{\rho_{hnf}/\rho_f}F'''+f_0F''+f_0''F-\chi F'-\frac{\eta}{2}\chi F''-2f_0'F'+\gamma F'=0, \tag{18}$$

$$\frac{k_{hnf}/k_f}{\Pr\left(\rho C_p\right)_{hnf}/\left(\rho C_p\right)_f}G''+\frac{QG}{\left(\rho C_p\right)_{hnf}/\left(\rho C_p\right)_f}+f_0G'+F\theta_0'-\frac{1}{2}\chi\eta G'+\gamma G=0, \tag{19}$$

correlate to

$$F(0)=0,\quad F'(0)=0,\quad G(0)=0,\quad F'(\infty)\to 0,\qquad G(\infty)\to 0. \tag{20}$$

One of the far fields $(\eta\to\infty)$ boundary conditions must be relaxed to identify the possible range of eigenvalues [27]. In this study, we opt for a relaxed boundary condition $F'(\infty)\to 0$, allowing for more flexibility in our analysis. As a result, we modify the system of Eq. (18) to Eq. (20) by incorporating the stabilizing boundary condition $F''(0)=1$. This adaptation aids us in effectively solving the equations and obtaining meaningful results.

4. Results and Discussion

To adequately analyse the flow problem, extensive numerical simulations were conducted in MATLAB using the bvp4c function. The bvp4c function in MATLAB employs finite difference coding to apply the three-stage Lobatto IIIa formula, which serves as a collocation method for solving boundary value problems involving systems of ordinary differential equations. To obtain solutions for the differential equations, an initial guess must be provided, which should closely approximate the specified boundary conditions. The aim of these simulations is to provide a comprehensive analysis of the physical aspects involved. To ensure the accuracy and reliability of our study, we compare the obtained results for the skin friction coefficient and the reduced Nusselt number with those obtained by Rohni *et al.,* [28] and Roy and Pop [29]. In their respective studies, Rohni *et al.,* [28] employed the shooting method, while Roy and Pop [29] combined the shooting method with the sixth-order Runge-Kutta method. The comparison, as shown in Table 3, reveals a significant level of agreement between the results, thus confirming the validity and effectiveness of the bvp4c function utilized in this investigation.

Table 3
Comparison values of $f''(0)$ and $-\theta'(0)$ for Cu-nanofluid with variation in χ when $\phi_1 = 0.2, \lambda = -1, Q = 0, \Pr = 6.2$ and $s = 2.1$

χ	$f''(0)$			$-\theta'(0)$		
	Roy and Pop [29]	Rohni *et al.*, [28]	Present	Roy and Pop [29]	Rohni *et al.*, [28]	Present
0.0	2.528971	2.5290	2.528983	6.822305	6.8225	6.822411
-0.2	-	2.4621	2.462145	-	6.7672	6.767187
-0.4	-	2.3953	2.395252	-	6.7120	6.711948
-0.6	-	2.3283	2.328304	-	6.6567	6.656694
-1.0	2.194299	2.1942	2.194246	7.073633	6.5462	6.546145
-3.0	1.521774	1.5212	1.521192	7.497279	5.9927	5.992657
-5.0	0.844960	0.8444	0.844435	7.858697	5.4382	5.438137

Figure 2 and Figure 3 present the distinct velocity and temperature profiles of single nanofluids containing only one type of nanoparticle, namely Cu-nanofluid $(\phi_1 = 0.02,\ \phi_2 = 0)$ and SiO_2-nanofluid $(\phi_1 = 0,\ \phi_2 = 0.02)$, as well as the Cu-$SiO_2$ hybrid nanofluid $(\phi_1 = \phi_2 = 0.02)$. In Figure 2, it is evident that the Cu-SiO_2 hybrid nanofluid exhibits the highest velocity profile, followed by Cu-nanofluid and SiO_2-nanofluid. This observation suggests that the presence of different nanoparticles in the hybrid nanofluid enhances fluid movement, leading to a reduction in the thickness of the momentum boundary layer. As shown in Figure 3, the Cu-SiO_2 hybrid nanofluid exhibits the lowest temperature, followed by SiO_2-nanofluid and Cu-nanofluid. This suggests that the hybrid nanofluid outperforms the single nanofluids in terms of heat dissipation. This finding aligns with the trend of the reduced Nusselt number illustrated in Figure 4, where the highest Nusselt number is achieved with the hybrid nanofluid. These findings collectively indicate that the hybrid nanofluid enables a more efficient heat transfer, owing to its thinner thermal boundary layer, thereby stimulating the heat transfer process.

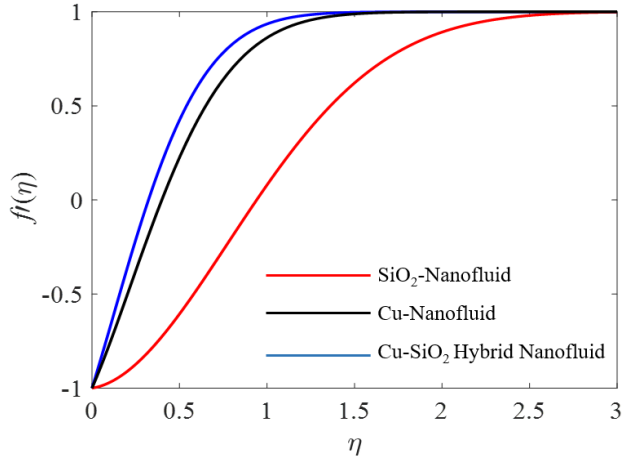

Fig. 2. Trend of velocity profiles for single nanofluid and hybrid nanofluid

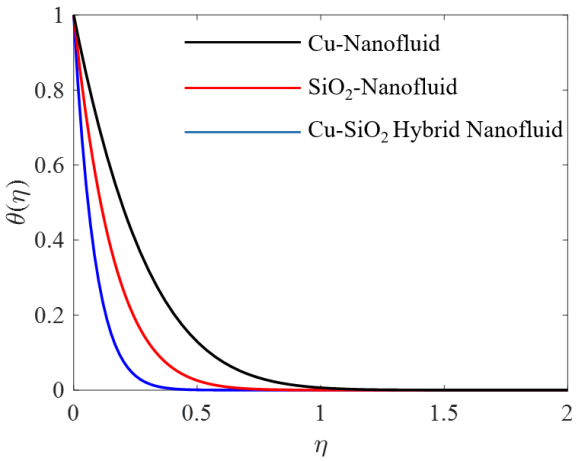

Fig. 3. Trend of temperature profiles for single nanofluid and hybrid nanofluid

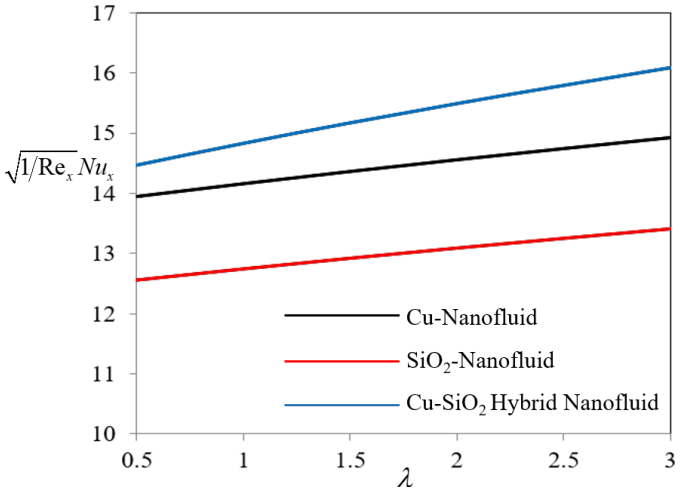

Fig. 4. Impact of single nanofluid and hybrid nanofluid to the Nusselt number

Suction, an effective technique for boundary layer control, plays a vital role in reducing drag on bodies exposed to external flows and minimizing energy losses in channels. By removing fluid from the boundary layer, suction creates a favorable pressure gradient that contributes to various benefits. One significant advantage is the reduction in boundary layer thickness, which directly translates to a decrease in drag experienced by the body. As depicted in Figure 5, the application of suction triggers an increase in the velocity gradient at the surface. This intensified velocity gradient leads to an elevation in wall shear stress, effectively diminishing the thickness of the momentum boundary layer. The reduction in the momentum boundary layer thickness enhances the fluid dynamics in the immediate vicinity of the surface, promoting more efficient flow characteristics. Additionally, Figure 6 sheds light on the impact of increased suction on the temperature distribution profile. It is observed that heightened suction levels cause a notable decrease in the temperature distribution, subsequently thinning the thermal boundary layer. This thinning of the thermal boundary layer facilitates an enhanced heat transfer process, allowing for a more efficient exchange of thermal energy between the surface and the surrounding fluid. Consequently, the overall heat transfer rate is improved, contributing to enhanced thermal performance.

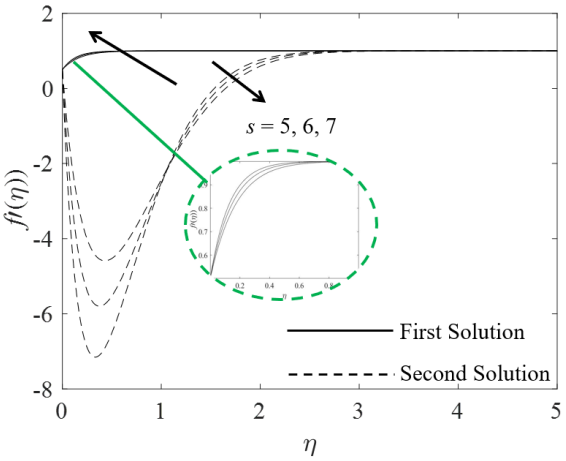

Fig. 5. Trend of $f'(\eta)$ with variation in s

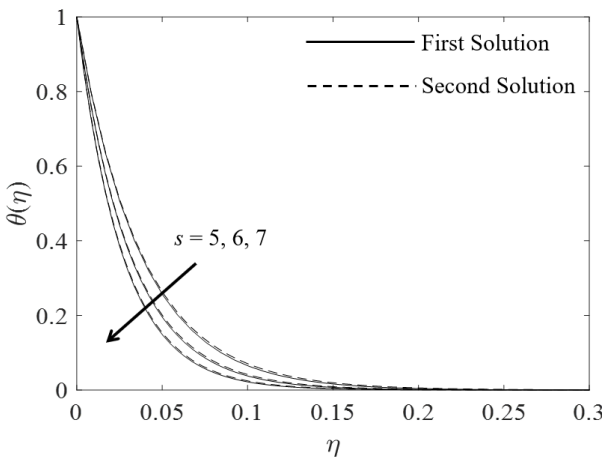

Fig. 6. Trend of $\theta(\eta)$ with variation in s

The effects of a heat source or sink on the hybrid nanofluid model is significant. Figure 7 demonstrates that the increment of heat source $(Q>0)$ which reflects the heat generation rises the hybrid nanofluid temperature. As a result, the value of the Nusselt number reduces as depicted in Figure 8. Conversely, Figure 9 illustrates the decrement of temperature as heat sink $(Q<0)$ which reflects the heat absorption intensifies, which in turn increases the value of Nusselt number as shown in Figure 10. When a heat source is present, it introduces thermal energy into the system, causing an increase in the temperature profile. On the other hand, the heat sink absorbs thermal energy from the system, resulting in a decrease in the temperature profile. The heat source/sink can modify the temperature distribution within the hybrid nanofluid, influencing the behaviour of the thermal boundary layer. As the heat source/sink intensity increases, the temperature gradient near the surface is altered, leading to changes in the thermal boundary layer thickness. In the case of a heat source, the thermal boundary layer tends to expand as the temperature rises, while a heat sink tends to thin the thermal boundary layer as the temperature decreases.

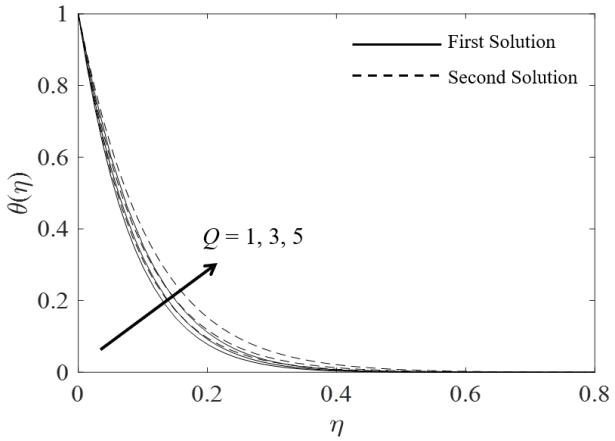

Fig. 7. Trend of $\theta(\eta)$ with variation in heat source $(Q>0)$

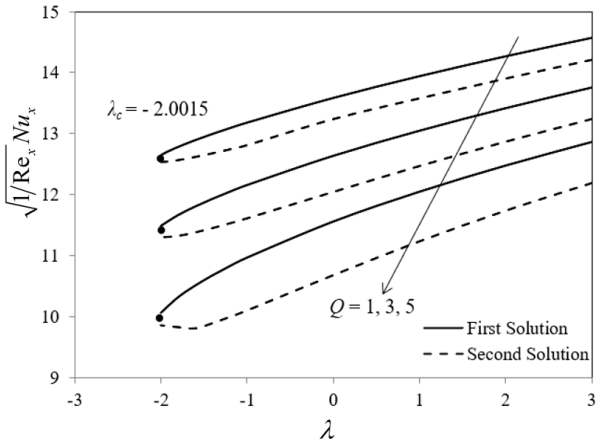

Fig. 8. Impact of heat source $(Q>0)$ to the Nusselt number

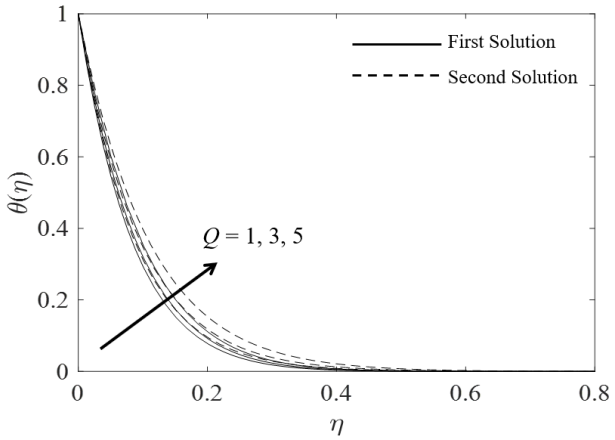

Fig. 9. Trend of $\theta(\eta)$ with variation in heat sink $(Q<0)$

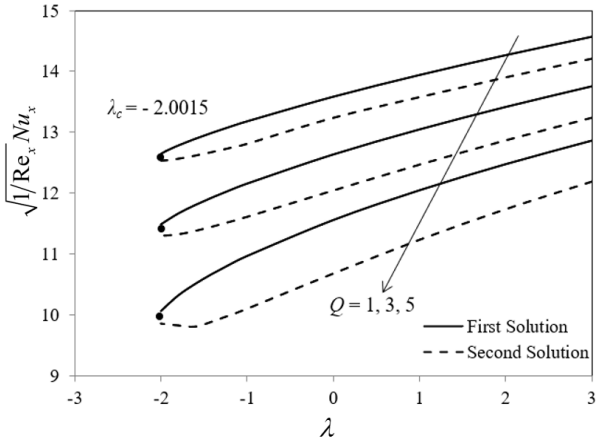

Fig. 10. Impact of heat sink $(Q<0)$ to the Nusselt number

The unsteadiness parameter plays a key role in unsteady flow and has a direct impact on the velocity profile and temperature profile. This parameter represents the degree of unsteadiness or time dependence in the flow. It quantifies how quickly the flow variables change with respect to time.

Figure 11 demonstrates how increasing the unsteadiness parameter results in a rise in velocity for the first solution, whereas a distinct pattern is shown for the second solution. The unsteadiness parameter affects the velocity profile by influencing the flow acceleration and deceleration. In regions where the unsteadiness parameter is high, the flow experiences rapid changes in velocity, leading to fluctuating flow patterns. These fluctuations can result in the formation of eddies, vortices, and flow instabilities. On the other hand, in regions with low unsteadiness parameter, the flow tends to be more uniform and steadier. Similarly, the unsteadiness parameter also influences the temperature profile. In unsteady flow, the temperature distribution can change rapidly due to the time-varying nature of the flow. Figure 12 portrays the depreciation of the thermal boundary layer thickness with the greater unsteadiness parameter. Unsteady flows typically exhibit enhanced convective heat transfer compared to steady flows. The fluctuating velocity field enhances the transport of heat away from the surface, facilitating a more efficient heat dissipation process. Consequently, the temperature at the surface decreases, leading to a reduced temperature profile.

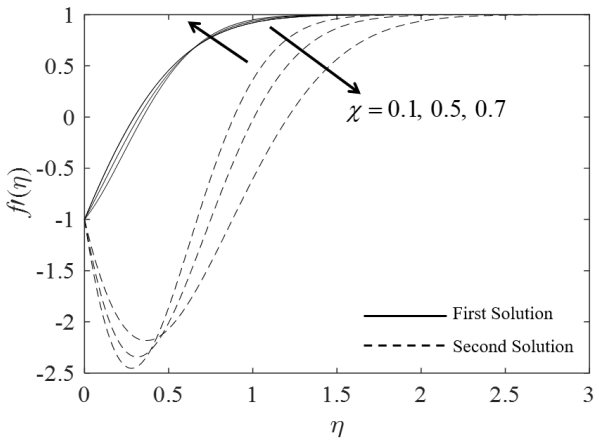

Fig. 11. Trend of $f'(\eta)$ with variation in χ

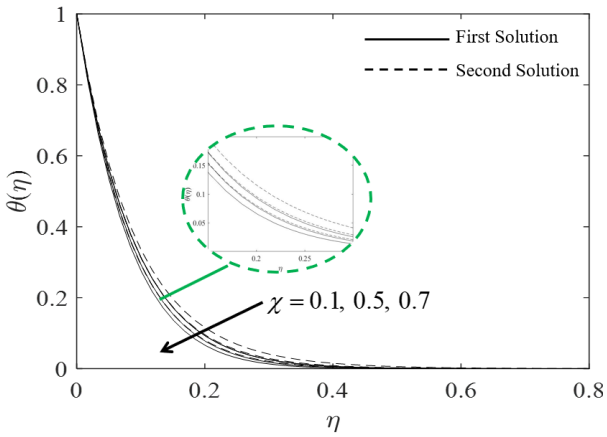

Fig. 12. Trend of $\theta(\eta)$ with variation in χ

A stability study is performed to evaluate the viability of the first and second solutions. This is done by figuring out the smallest eigenvalue γ_1 and solving the eigenvalue problems (18) through (20). The smallest eigenvalue, γ_1, is produced as part of an infinite collection of eigenvalues $\gamma_1 < \gamma_2 < \gamma_3 \ldots$. If the flow is unstable and the smallest eigenvalue is negative, this means the disturbances have increased. On the contrary, a positive smallest eigenvalue denotes a decrease in disturbances and reflects the flow stability. The first solution is found to be stable, as illustrated in Figure 13, while the second solution is discovered to be unstable.

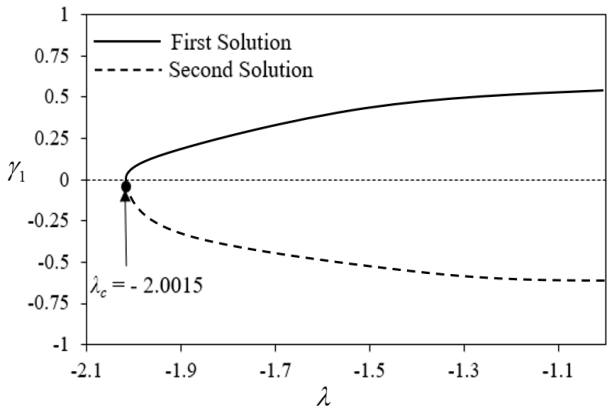

Fig. 13. Values γ_1 with λ

5. Conclusions

This study investigated the influence of heat generation/absorption on the unsteady Hiemenz flow and heat transfer of Cu-SiO_2 hybrid nanofluid. The numerical findings made significant contributions to understanding the flow characteristics and heat transfer behavior of hybrid nanofluid. The results demonstrated that employing a hybrid nanofluid enhances the rate of heat transfer compared to using a single nanofluid. The introduction of suction led to an augmentation in the velocity distribution profile and a reduction in the thickness of the momentum boundary layer, consequently affecting the temperature profile. Additionally, heat absorption facilitated greater heat dissipation, while heat generation impeded the heat transfer process. Furthermore, the unsteadiness parameter played a role in thinning both the momentum and thermal boundary layer thicknesses. The study revealed the existence of dual solutions, indicating the presence of multiple flow regimes. Through stability analysis, it was confirmed that the first solution exhibited stable behavior, conforming to the expected stability characteristics.

Acknowledgement
The authors would like to express their appreciation to Universiti Malaysia Pahang Al-Sultan Abdullah for providing financial support through research grants RDU223202 and RDU213201, which greatly contributed to the completion of this work.

References

[1] Ling, Y., A. Haselbacher, and S. Balachandar. "Importance of unsteady contributions to force and heating for particles in compressible flows: Part 1: Modeling and analysis for shock-particle interaction." *International Journal of Multiphase Flow* 37, no. 9 (2011): 1026-1044. https://doi.org/10.1016/j.ijmultiphaseflow.2011.07.001
[2] Azoury, P. H. *Engineering applications of unsteady fluid flow*. Wiley, 1992.
[3] Bilal, M., M. Safdar, S. Ahmed, and R. Ahmad Khan. "Analytic similarity solutions for fully resolved unsteady laminar boundary layer flow and heat transfer in the presence of radiation." *Heliyon* 9, no. 4 (2023). https://doi.org/10.1016/j.heliyon.2023.e14765
[4] Kandasamy, R., I. Muhaimin, Azme B. Khamis, and Rozaini bin Roslan. "Unsteady Hiemenz flow of Cu-nanofluid over a porous wedge in the presence of thermal stratification due to solar energy radiation: Lie group transformation." *International Journal of Thermal Sciences* 65 (2013): 196-205. https://doi.org/10.1016/j.ijthermalsci.2012.10.013
[5] Mahmood, Asad, Bin Chen, and Abuzar Ghaffari. "Hydromagnetic Hiemenz flow of micropolar fluid over a nonlinearly stretching/shrinking sheet: Dual solutions by using Chebyshev Spectral Newton Iterative Scheme." *Journal of Magnetism and Magnetic Materials* 416 (2016): 329-334. https://doi.org/10.1016/j.jmmm.2016.05.001
[6] Waini, Iskandar, Anuar Ishak, and Ioan Pop. "Hiemenz flow over a shrinking sheet in a hybrid nanofluid." *Results in Physics* 19 (2020): 103351. https://doi.org/10.1016/j.rinp.2020.103351
[7] Bakar, Shahirah Abu, Norihan Md Arifin, and Ioan Pop. "Stability Analysis on Mixed Convection Nanofluid Flow in a Permeable Porous Medium with Radiation and Internal Heat Generation." *Journal of Advanced Research in Micro and Nano Engineering* 13, no. 1 (2023): 1-17. https://doi.org/10.37934/armne.13.1.117
[8] Saidin, Norshaza Atika, Mohd Ariff Admon, and Khairy Zaimi. "Unsteady Three-Dimensional Free Convection Flow Near the Stagnation Point Over a General Curved Isothermal Surface in a Nanofluid." *CFD Letters* 12, no. 6 (2020): 80-92. https://doi.org/10.37934/cfdl.12.6.8092
[9] Akaje, Wasiu, and B. I. Olajuwon. "Impacts of Nonlinear thermal radiation on a stagnation point of an aligned MHD Casson nanofluid flow with Thompson and Troian slip boundary condition." *Journal of Advanced Research in Experimental Fluid Mechanics and Heat Transfer* 6, no. 1 (2021): 1-15.
[10] Khan, Umair, Aurang Zaib, Sakhinah Abu Bakar, and Anuar Ishak. "Unsteady stagnation-point flow of a hybrid nanofluid over a spinning disk: analysis of dual solutions." *Neural Computing and Applications* 34, no. 10 (2022): 8193-8210. https://doi.org/10.1007/s00521-022-06916-z
[11] Maiti, Hiranmoy, Amir Yaseen Khan, Sabyasachi Mondal, and Samir Kumar Nandy. "Scrutinization of unsteady MHD fluid flow and entropy generation: Hybrid nanofluid model." *Journal of Computational Mathematics and Data Science* 6 (2023): 100074. https://doi.org/10.1016/j.jcmds.2023.100074

[12] Lahari, M. L. R. Chaitanya, P. H. V. Sesha Talpa Sai, K. V. Sharma, and K. S. Narayanaswamy. "Thermal conductivity and viscosity of glycerine-water based Cu-SiO_2 hybrid nanofluids." *Materials Today: Proceedings* 66 (2022): 1823-1829. https://doi.org/10.1016/j.matpr.2022.05.284

[13] Dezfulizadeh, Amin, Alireza Aghaei, Ali Hassani Joshaghani, and Mohammad Mahdi Najafizadeh. "An experimental study on dynamic viscosity and thermal conductivity of water-Cu-SiO_2-MWCNT ternary hybrid nanofluid and the development of practical correlations." *Powder Technology* 389 (2021): 215-234. https://doi.org/10.1016/j.powtec.2021.05.029

[14] Masood, Sadaf, Muhammad Farooq, and Aisha Anjum. "Influence of heat generation/absorption and stagnation point on polystyrene-TiO_2/H_2O hybrid nanofluid flow." *Scientific Reports* 11, no. 1 (2021): 22381. https://doi.org/10.1038/s41598-021-01747-9

[15] Yasir, Muhammad, Masood Khan, A. S. Alqahtani, and M. Y. Malik. "Heat generation/absorption effects in thermally radiative mixed convective flow of Zn− TiO_2/H_2O hybrid nanofluid." *Case Studies in Thermal Engineering* 45 (2023): 103000.

[16] Rashad, Ahmed M., Mohamed A. Nafe, and Dalia A. Eisa. "Heat generation and thermal radiation impacts on flow of magnetic Eyring-Powell hybrid nanofluid in a porous medium." *Arabian Journal for Science and Engineering* 48, no. 1 (2023): 939-952. https://doi.org/10.1007/s13369-022-07210-9

[17] Iftikhar, Naheeda, Abdul Rehman, and Hina Sadaf. "Theoretical investigation for convective heat transfer on Cu/water nanofluid and (SiO_2-copper)/water hybrid nanofluid with MHD and nanoparticle shape effects comprising relaxation and contraction phenomenon." *International Communications in Heat and Mass Transfer* 120 (2021): 105012. https://doi.org/10.1016/j.icheatmasstransfer.2020.105012

[18] Zainal, Nurul Amira, Roslinda Nazar, Kohilavani Naganthran, and Ioan Pop. "Unsteady stagnation point flow of hybrid nanofluid past a convectively heated stretching/shrinking sheet with velocity slip." *Mathematics* 8, no. 10 (2020): 1649. https://doi.org/10.3390/math8101649

[19] Jusoh, Rahimah, Roslinda Nazar, and Ioan Pop. "Impact of heat generation/absorption on the unsteady magnetohydrodynamic stagnation point flow and heat transfer of nanofluids." *International Journal of Numerical Methods for Heat & Fluid Flow* 30, no. 2 (2020): 557-574. https://doi.org/10.1108/HFF-04-2019-0300

[20] Takabi, Behrouz, and Saeed Salehi. "Augmentation of the heat transfer performance of a sinusoidal corrugated enclosure by employing hybrid nanofluid." *Advances in Mechanical Engineering* 6 (2014): 147059. https://doi.org/10.1155/2014/147059

[21] Hussain, S., Sameh E. Ahmed, and T. Akbar. "Entropy generation analysis in MHD mixed convection of hybrid nanofluid in an open cavity with a horizontal channel containing an adiabatic obstacle." *International Journal of Heat and Mass Transfer* 114 (2017): 1054-1066. https://doi.org/10.1016/j.ijheatmasstransfer.2017.06.135

[22] Bhatti, M. M., Hakan F. Öztop, R. Ellahi, Ioannis E. Sarris, and Mohammad Hossein Doranehgard. "Insight into the investigation of diamond (C) and Silica (SiO_2) nanoparticles suspended in water-based hybrid nanofluid with application in solar collector." *Journal of Molecular Liquids* 357 (2022): 119134. https://doi.org/10.1016/j.molliq.2022.119134

[23] Merkin, J. H. "On dual solutions occurring in mixed convection in a porous medium." *Journal of Engineering Mathematics* 20, no. 2 (1986): 171-179. https://doi.org/10.1007/BF00042775

[24] Merrill, Keith, Matthew Beauchesne, Joseph Previte, Joseph Paullet, and Patrick Weidman. "Final steady flow near a stagnation point on a vertical surface in a porous medium." *International Journal of Heat and Mass Transfer* 49, no. 23-24 (2006): 4681-4686. https://doi.org/10.1016/j.ijheatmasstransfer.2006.02.056

[25] Kho, Yap Bing, Rahimah Jusoh, Mohd Zuki Salleh, Mohd Hisyam Ariff, and Nooraini Zainuddin. "Magnetohydrodynamics Ag-Fe_3O_4-Ethylene Glycol Hybrid Nanofluid Flow and Heat Transfer with Thermal Radiation." *CFD Letters* 14, no. 11 (2022): 88-101. https://doi.org/10.37934/cfdl.14.11.88101

[26] Weidman, P. D., D. G. Kubitschek, and A. M. J. Davis. "The effect of transpiration on self-similar boundary layer flow over moving surfaces." *International Journal of Engineering Science* 44, no. 11-12 (2006): 730-737. https://doi.org/10.1016/j.ijengsci.2006.04.005

[27] Harris, S. D., D. B. Ingham, and I. Pop. "Mixed convection boundary-layer flow near the stagnation point on a vertical surface in a porous medium: Brinkman model with slip." *Transport in Porous Media* 77 (2009): 267-285. https://doi.org/10.1007/s11242-008-9309-6

[28] Rohni, Azizah Mohd, Syakila Ahmad, and Ioan Pop. "Flow and heat transfer over an unsteady shrinking sheet with suction in nanofluids." *International Journal of Heat and Mass Transfer* 55, no. 7-8 (2012): 1888-1895. https://doi.org/10.1016/j.ijheatmasstransfer.2011.11.042

[29] Roy, Nepal Chandra, and Ioan Pop. "Unsteady magnetohydrodynamic stagnation point flow of a nanofluid past a permeable shrinking sheet." *Chinese Journal of Physics* 75 (2022): 109-119. https://doi.org/10.1016/j.cjph.2021.12.018